Journal of Tribology

Technical Briefs

A Compact Model for Spherical Rough Contacts

M. Bahrami
Post Doctoral Fellow
Member ASME
e-mail: majid@mhtlab.uwaterloo.ca

M. M. Yovanovich
Distinguished Professor Emeritus
Fellow ASME

J. R. Culham
Associate Professor
Director
Member ASME

Microelectronics Heat Transfer Laboratory, Dept. of Mechanical Engineering, University of Waterloo, Waterloo, ON N2L 3G1, Canada

A new model is developed that considers the effect of roughness on the elastic contact of spherical bodies. A general pressure distribution is proposed that encompasses the contact of rough spheres and yields the Hertzian theory for ideally smooth surfaces. A new parameter, nondimensional maximum contact pressure, is introduced and it is shown that this is the key parameter that controls the contact. The results of the present study are presented in the form of compact relationships. These relationships are compared against the experimental data collected by others and good agreement is observed. [DOI: 10.1115/1.2000982]

Introduction

Hertzian theory is based on the premise that the contacting surfaces are ideally smooth and thus perfect contact takes place throughout the nominal contact area. However, real surfaces have roughness and contact occurs only at discrete spots called microcontacts where asperities make contact. The real contact area is usually a small fraction of the nominal contact area. Hertz replaced the contacting spheres with paraboloids; thus the contact between two spheres was simplified to the contact of a plane and a profile that has an effective radius of curvature ρ, where $1/\rho = 1/\rho_1 + 1/\rho_2$. For convenience, all elastic deformations can be considered to occur in one body, which has an effective elastic modulus E', and the other body is assumed to be rigid; where

$$\frac{1}{E'} = \frac{1-\nu_1^2}{E_1} + \frac{1-\nu_2^2}{E_2} \tag{1}$$

Hertz proposed the following pressure distribution [1]:

$$P_H(r/a_H) = P_{0,H}\sqrt{1-(r/a_H)^2} \tag{2}$$

where $P_{0,H}=1.5F/(\pi a_H^2)$ and $a_H=(0.75F\rho/E')^{1/3}$ are the maximum pressure and the radius of the Hertzian contact area, respectively.

If roughness is isotropic and randomly distributed, the surface is called Gaussian. Williamson et al. [2] have shown experimentally that many of the techniques used to produce engineering surfaces give a Gaussian distribution of surface heights. Many engineering surfaces do not follow a symmetric Gaussian distribution but rather an asymmetric distribution [3]. However, in this study we focus only on Gaussian surfaces.

Literature Review

The literature contains very few analytical models for the contact of spherical rough surfaces. Contact of rough spheres includes two problems, (i) the bulk compression and (ii) deformation of asperities.

Different approaches have been taken to analyze the deformation of asperities by assuming plastic [4], elastic [5], elastoplastic [6,7] regimes at microcontacts. It has been observed through experiments that the real contact area is proportional to the load [8]. However, if elastic deformation is assumed for asperities, using the Hertzian theory, the real contact area will not be linearly proportional to the load, instead one obtains $A_r \propto F^{2/3}$. Archard [9] solved this problem by proposing that the surface asperities have micro-asperities and micro-asperities have micro-micro asperities and so on, by adding several levels of asperities, Archard showed that $A_r \propto F$. Greenwood and Williamson (GW) [5] subsequently developed an elastic contact model; the GW model also satisfied the observed proportionality $A_r \propto F$. As a result, an *effective elastic microhardness* can be defined for elastic models which shows that the assumption of elastic and/or plastic deformation of asperities leads to similar results [5,10]. Greenwood and Williamson [5] introduced a plasticity index as a criterion for plastic flow of microcontacts. They reported that the load has little effect on the deformation regime. Based on the plasticity index, they concluded that except for especially smooth surfaces, the asperities will flow plastically under the lightest loads. Considering an indentation hardness for asperities, Persson [11] also concluded that except for polished surfaces all microcontacts deform plastically.

The GW [5] elastic model postulates asperities with a constant radius of curvature β and a Gaussian distribution of heights. Moreover, the GW model assumes that asperities entirely deform elastically, i.e., Hertzian theory can be applied for each individual summit. According to the GW model, the summits or "peaks" on a surface profile are the points higher than their immediate neighbors at the sampling interval used. Recently Greenwood and Wu

Contributed by the Tribology Division of ASME for publication in the ASME JOURNAL OF TRIBOLOGY. Manuscript received July 15, 2004; Final manuscript received April 29, 2005. Review conducted by: Michael Lovell.

[12] reviewed the assumptions of the GW model and concluded that "the GW definition of peaks is wrong and gives a false idea of both the number and the radius of curvature of asperities." Greenwood and Wu proposed to return to the Archard idea that roughness consists of roughness on roughness and that the contact may be plastic at light loads but it becomes elastic at heavier loads. Based on the fractal characterization, Majumdar and Bhushan [13] developed a model for contact between two isotropic rough surfaces. According to their model, smaller asperities have smaller radii of curvature and, therefore, are more likely to undergo plastic deformation. By increasing the load, these small plastic deformations join to form elastic contact spots.

Greenwood and Tripp (GT) [10] performed the first analytical study to investigate the effect of roughness on elastic spherical bodies. The GT model shares the same assumptions as the GW model for microcontacts. Moreover, the bulk deformation was assumed to be elastic. The elastic deformation produced by an axially symmetric pressure distribution over a circular area on a half-space can be found from [10,14]

$$\omega_b(r) = \begin{cases} \dfrac{2}{E'}\displaystyle\int_0^\infty P(s)ds & r = 0 \\ \dfrac{4}{\pi E' r}\displaystyle\int_0^r sP(s)K\left(\dfrac{s}{r}\right)ds & r > s \\ \dfrac{4}{\pi E'}\displaystyle\int_r^\infty P(s)K\left(\dfrac{r}{s}\right)ds & r < s \end{cases} \tag{3}$$

where $K(\cdot)$ is the complete elliptic integral of the first kind and a is the radius of the circle. Greenwood and Tripp [10] presented a set of relationships and showed the results of their numerical model. The GT analysis were reported to be primarily a function of a nondimensional parameter $T=2F/\sigma E'\sqrt{2\rho\sigma}$ and a weak function of another nondimensional parameter $\mu=8\sigma\eta\sqrt{2\rho\beta}/3$. The most important trends in the GT model were that an increase in roughness resulted in a decrease in the pressure and an increase in the contact area.

Mikic and Roca [15] developed an alternative numerical model by assuming plastic deformation of asperities. Similar trends to those of the GT model were presented graphically. The modeling results of [15] were also mainly a function of a nondimensional parameter $\bar{\sigma}=\pi\sigma E'/a_H P_H$ and a weak function of H/P_H, where P_H was the average pressure in the Hertzian limit. Kagami et al. [16] developed a numerical model for spherical rough contacts and conducted experiments to verify their model. They assumed that the asperities with deformations below and above a critical value were deformed elastically and plastically, respectively. They showed through comparison with their data that the effect of the deformation mode of asperities, i.e., elastic, plastic, or elastoplastic was small in the practical range. Greenwood et al. [17] introduced a nondimensional roughness parameter, α, as

$$\alpha = \frac{\sigma\rho}{a_H^2} = \sigma\left(\frac{16\rho E'^2}{9F^2}\right)^{1/3} \tag{4}$$

Greenwood et al. [17] showed that the controlling nondimensional parameters in both elastic [10] and plastic [15] models can be written in terms of α, i.e., $T=4\sqrt{2}/3\sqrt{\alpha^3}$ and $\bar{\sigma}=3\pi^2\alpha/4$, respectively. They concluded, for rough spherical contacts, it is unimportant whether the asperities deform elastically or plastically; the contact pressure is predominantly governed by α. Further, if the value of α is less than 0.05, the effect of roughness is negligible and the Hertzian theory can be used.

As discussed above, the existing models have the following limitations: (i) They are presented as sets of relationships; applying these models is complex and requires intensive numerical computations. None of the existing models offer relationships for the contact parameters. (ii) A general pressure distribution that accounts for surface roughness does not exist in the literature. Pressure distribution is essential for thermal and electrical contact resistance analyses. The objective of this paper is to develop a compact model that predicts the contact parameters without going through complex numerical computations.

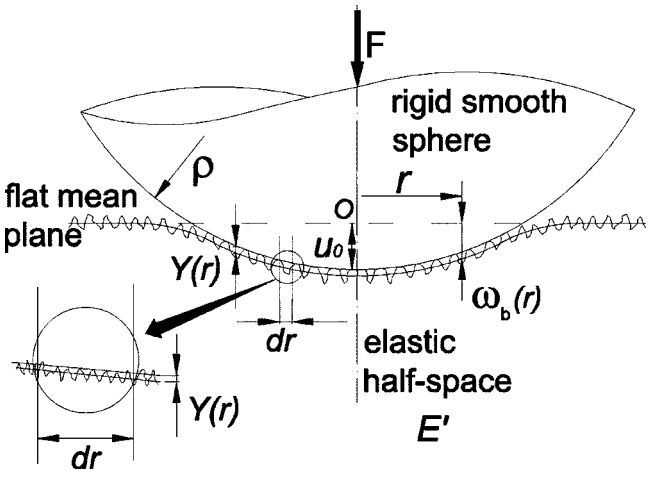

Fig. 1 Contact between sphere and rough plane

Present Model

The deformation mode of asperities is assumed to be plastic. Assuming plastically deformed microcontacts, Cooper et al. [4] derived a relationship for the real contact area for contact of conforming rough surfaces

$$\frac{A_r}{A_a} = \frac{1}{2}\,\mathrm{erfc}\,\lambda \tag{5}$$

where $\lambda = Y/\sqrt{2}\sigma$, Y, and $\mathrm{erfc}(\cdot)$ are the nondimensional separation, separation between mean planes, and complementary error function, respectively.

The substrate deformation is assumed to be elastic. The geometry of the contact is shown in Fig. 1. All the bulk deformations are assumed to occur in the elastic half-space which has an effective elasticity modulus E'. Discrete point forces are created at the contact spots where the pressure is the microhardness of the softer of the two materials in contact. The surface roughness acts like a plastic layer on an elastic half-space, in the sense that the effect of these point forces on the elastic half-space is considered as a continuous pressure $P(r)$. A schematic free-body diagram of the contact is shown in Fig. 2. As a result of surface curvature, the

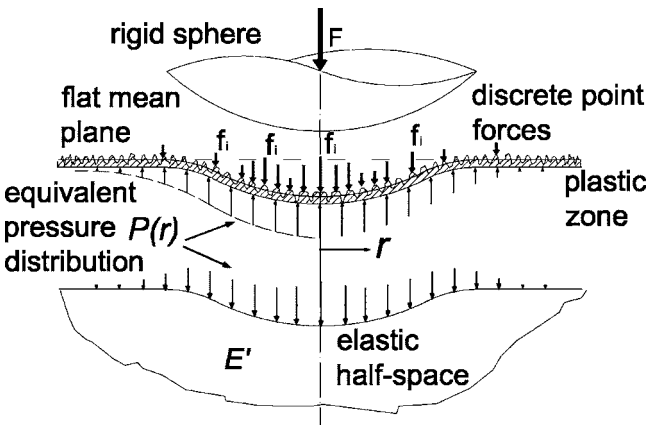

Fig. 2 Free-body diagram of contact, discrete point forces and plastic layer

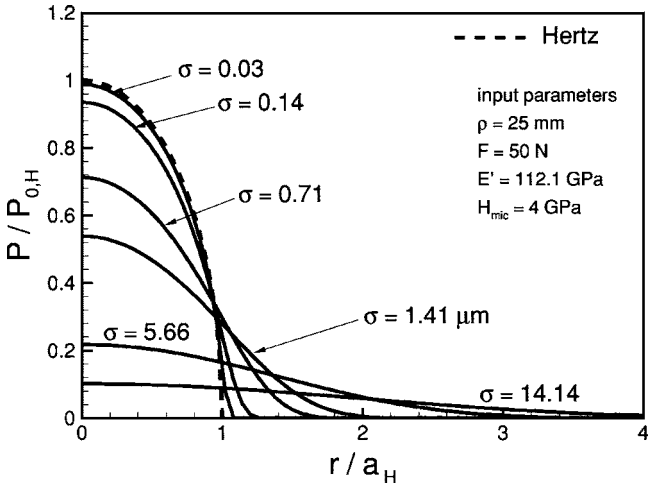

Fig. 3 Effect of roughness on pressure distribution

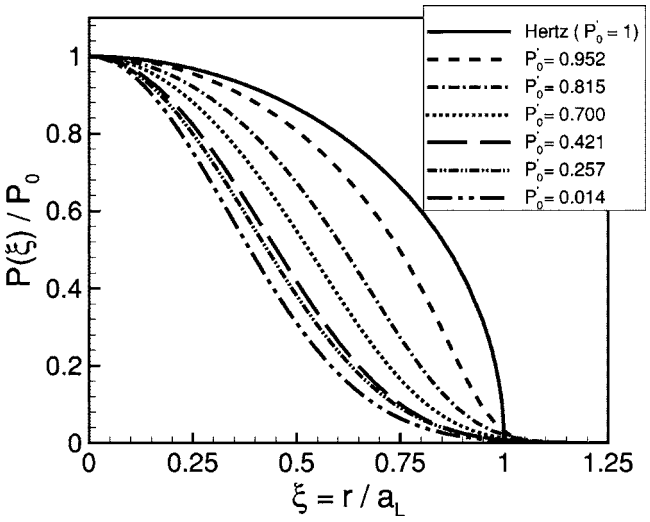

Fig. 4 Nondimensional pressure distributions for spherical rough contacts

separation and consequently the mean size and the number of the microcontacts vary with radial position. In an infinitesimal surface element dr, the local separation $Y(r)$ is uniform, see Fig. 1. Therefore, the conforming rough contact relationship Eq. (5), can be applied to determine the ratio of the real to apparent area

$$\frac{dA_r(r)}{dA_a(r)} = \frac{1}{2}\,\text{erfc}\,\lambda(r) \tag{6}$$

where $dA_a(r)=2\pi r dr$. In the vicinity of the contact, the profile of the sphere is approximated by a paraboloid, $u(r)=u_0-r^2/2\rho$. The local separation $Y(r)$ is the distance between two mean planes of the contacting surfaces which can be written as

$$Y(r) = \omega_b(r) - u(r) = \omega_b(r) - u_0 + r^2/2\rho \tag{7}$$

Depending on the surface preparation and the machining process, microhardness can have a greater value than the bulk hardness [11]. However, in this study, an effective microhardness H_{mic} is considered which is constant throughout the contact region.

The external load F is the summation of the point forces acting at the microcontacts, see Fig. 2

$$F = \sum_i \text{f}_i = H_{\text{mic}} \int_{\text{contact area}} \int dA_r(r) \tag{8}$$

Combining Eqs. (6) and (8) and considering a circular contact area, one obtains

$$F = \pi H_{\text{mic}} \int_0^\infty \text{erfc}\,\lambda(r)\; r dr \tag{9}$$

The upper limit of the integral is set to infinity and that is because the effective pressure distribution rapidly approaches zero at the edge of the contact area, thus it will not affect the final solution. On the bulk side, the contact pressure must also satisfy the force balance, thus, the pressure distribution is

$$P(r) = \tfrac{1}{2} H_{\text{mic}}\,\text{erfc}\,\lambda(r) \tag{10}$$

The elastic displacement of the half-space can be found by substituting the pressure distribution Eq. (10) into Eq. (3). Equations (3), (5), (7), (9), and (10) form a closed set of governing relationships. An algorithm and a computer program were developed to solve the set numerically. The numerical solution involves removing singularities and instabilities. Under-relaxation techniques have been extensively employed to stabilize the convergence, especially when approaching the Hertzian limit, for more detail see [18].

Figure 3 shows the effect of roughness on the pressure distribution predicted by the model for a typical stainless steel rough sphere-flat contact. The program was run for a wide range of roughness values while other input parameters shown in Fig. 3 were kept constant. As shown, increasing roughness results in a decrease in the maximum contact pressure and spreads the load over a larger area. Also the contact pressure approaches the Hertzian pressure as roughness approaches zero.

The contact area is the area where the microcontacts are distributed; also the contact pressure falls off to a negligible value (zero in the Hertzian limit) at the edge of the contact area. Unlike the Hertzian contact, in contact of rough spheres, the pressure distribution approaches zero asymptotically. As a result, the contact radius is not an exact point and its definition is rather arbitrary [1,10]. In this study, the contact radius is considered as the radius where the normalized pressure is negligible, i.e., $P(r=a_L)/P_0 < 0.01$.

General Pressure Distribution

Figure 4 illustrates several nondimensional pressure distributions predicted by the model for some values of $P_0'=P_0/P_{0,H}$ versus the nondimensional radial location $\xi=r/a_L$. As shown, a general profile exists that covers all spherical rough contacts. The pressure distribution profile, especially in the contacts where P_0' is less than 0.6, is very similar to a Gaussian distribution. However, as P_0' approaches unity (the Hertzian contact) the pressure distribution profile begins to deviate from the Gaussian profile. After considerable investigation, we found the following profile:

$$P(\xi) = P_0(1-\xi^2)^\gamma \tag{11}$$

where γ is calculated through a force balance to be

$$\gamma = 1.5\frac{P_0}{P_{0,H}}\left(\frac{a_L}{a_H}\right)^2 - 1 \tag{12}$$

Also the relationship between the maximum pressure P_0 and the applied force F is, $P_0=(1+\gamma)F/(\pi a_L^2)$. In the limit where roughness approaches zero, both P_0' and a_L' approach unity and $\gamma=0.5$; thus Eq. (11) yields the Hertzian pressure distribution, i.e., Eq. (2). With the general pressure distribution profile, Eq. (11), the problem is reduced to finding relationships for P_0 and a_L. Further, the radius of the contact area, based on its definition, can be found if P_0 and the pressure distribution are known; therefore, the key parameter is the maximum contact pressure P_0.

Scaling down Eqs. (7) and (10) and using a force balance and Eq. (3), one finds that the solution depends on two nondimen-

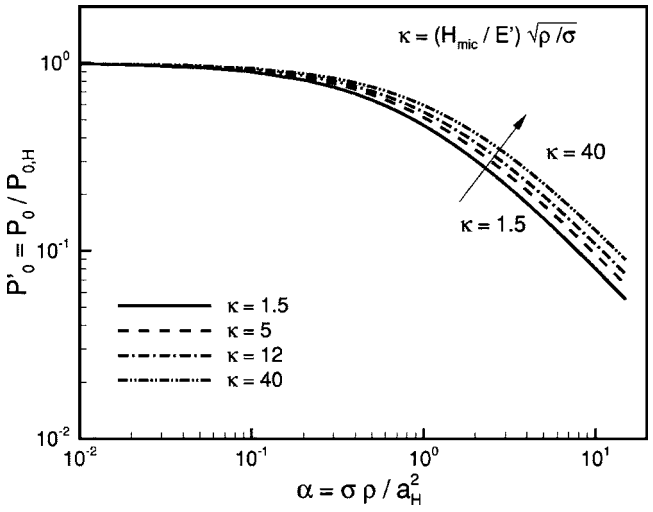

Fig. 5 Nondimensional maximum contact pressure

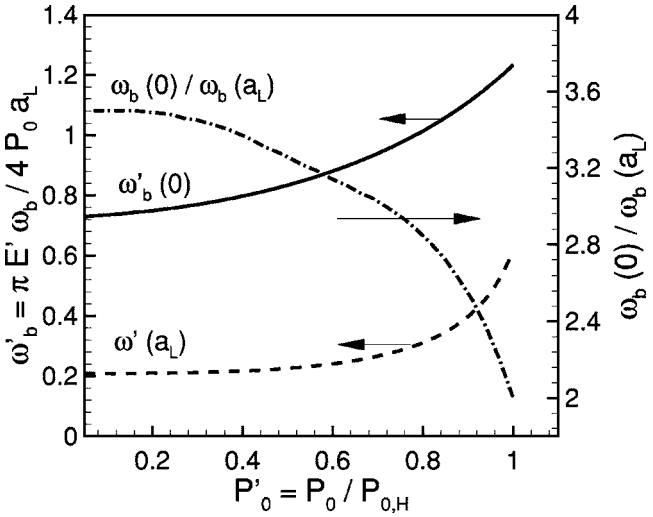

Fig. 6 Bulk deformation at center and edge of contact area

sional parameters. One can be written in terms of the roughness parameter α, introduced by [17] and the other is:

$$\kappa = \frac{E'}{H_{\text{mic}}}\sqrt{\frac{\rho}{\sigma}} \tag{13}$$

The present model was run for a wide range of nondimensional parameters α and κ to construct Fig. 5. As shown, P_0' is governed predominantly by the roughness parameter α and the parameter κ has a minor role. As expected, by decreasing α, P_0' approaches unity (the Hertzian contact). The nondimensional maximum contact pressure P_0' and the contact radius a_L' are curve fitted and the following are proposed:

$$P_0' = \frac{1}{1 + 1.22\alpha\kappa^{-0.16}} \tag{14}$$

$$a_L' = \begin{cases} 1.605/\sqrt{P_0'} & 0.01 \leqslant P_0' \leqslant 0.47 \\ 3.51 - 2.51P_0' & 0.47 \leqslant P_0' \leqslant 1 \end{cases} \tag{15}$$

The difference between Eqs. (14) and (15) and the full model is estimated to be less than 5% in the range of $0.01 \leqslant P_0' \leqslant 1$.

As the applied load increases, α decreases; thus the effect of roughness on the contact becomes smaller, see Fig. 5. For most practical applications, the effect of roughness is already negligible when the bulk deformation passes the elastic limit and the elastoplastic region. This is in agreement with the elastic deformation assumption for the substrate.

Bulk Deformation

The elastic deformation of the half-space can be calculated by substituting the general pressure distribution Eq. (11) into Eq. (3), where the radius of the contact area is a_L:

$$\omega_b'(\xi) = \begin{cases} \dfrac{\pi}{2}\displaystyle\int_0^1 (1-s^2)^\gamma ds & \xi = 0 \\ \dfrac{1}{\xi}\displaystyle\int_0^\xi s(1-s^2)^\gamma K\left(\frac{s}{\xi}\right) ds & s < \xi \\ \displaystyle\int_\xi^1 (1-s^2)^\gamma K\left(\frac{\xi}{s}\right) ds & s > \xi \end{cases} \tag{16}$$

where $\omega_b' = \pi E' \omega_b/(4P_0 a_L)$ is the nondimensional bulk deformation. Analytical solutions cannot be found for the second and third integrals in Eq. (16); thus they have been solved numerically for values of γ. The solution at the edge of the contact area ($\xi = 1$) has been correlated and the following relationship is proposed:

$$\omega_b(a_L) = \frac{4P_0 a_L}{\pi E'[4.79 - 3.17(P_0')^{3.13}]} \tag{17}$$

The maximum difference between Eq. (17) and the numerical solution is approximately 4.6%. In the Hertzian limit, elastic deformations of the half-space at the center and the edge of the contact area are: $\omega_{b,H}(0) = a_H^2/\rho$ and $\omega_{b,H}(a_H) = a_H^2/2\rho$, respectively. It can be seen that in the Hertzian limit, Eqs. (16) and (17) yield the Hertzian values, respectively. Figure 6 shows nondimensional deformations at the center $\omega_b'(0)$ and at the edge of the contact area $\omega_b'(a_L)$. In addition, the ratio of these deformations is shown in the plot over a wide range of P_0'. As the nondimensional maximum pressure decreases, i.e., the effect of roughness becomes more significant, bulk deformations at both the center and the edge of the contact decrease. As shown in Fig. 6, the ratio of deformations, $\omega_b(0)/\omega_b(a_L)$, increases as the nondimensional maximum pressure P_0' decreases. In other words, the ratio of $\omega_b(0)/\omega_b(a_L)$ is larger for "rougher" contacts which is a direct result of the contact pressure, i.e., the general pressure falls off faster than the Hertzian pressure, see Fig. 4.

The term compliance has been used in different ways. In this study, Kagami et al. [16] definition has been adopted since it allows us to verify the model with [16] data. Compliance between rough spheres is a function of asperity deformation $\omega_a(r)$, bulk deformation $\omega_b(r)$, and radial location and sphere radius; it is defined as [16]:

$$\delta = a_L^2/2\rho + \omega_b(a_L) \tag{18}$$

Combining Eqs. (15), (17), and (18), one obtains

$$\delta' = \frac{\delta}{\delta_H} = 0.5(a_L')^2 + \frac{8P_0'a_L'}{\pi^2[4.79 - 3.17(P_0')^{3.13}]} \tag{19}$$

where $\delta_H = a_H^2/\rho$. Equation (19) is plotted in Fig. 9 for a range of P_0'. In the limit where roughness approaches zero, P_0' and a_L' both approach unity and $\delta' = 1$ (the Hertzian value).

Comparison with Experimental Data

The results of the present model have been used in a thermal analysis to predict the thermal contact resistance (TCR) of spherical rough contacts in a vacuum. The developed model showed very good agreement with more than 280 experimental data points collected by many researchers during the last forty years [19].

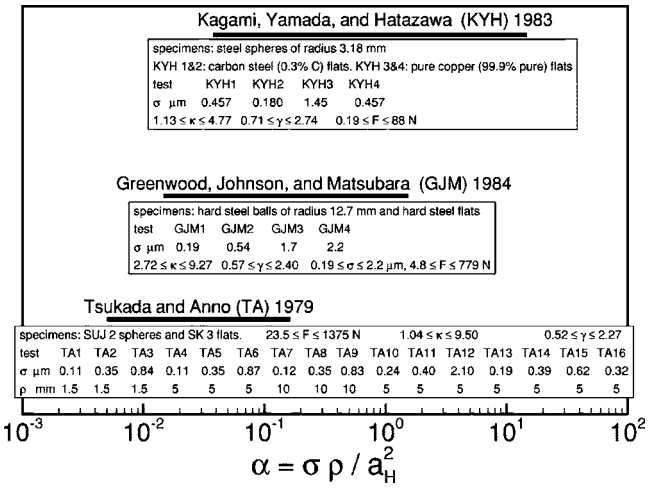

Fig. 7 Summary of parameter values of experimental data

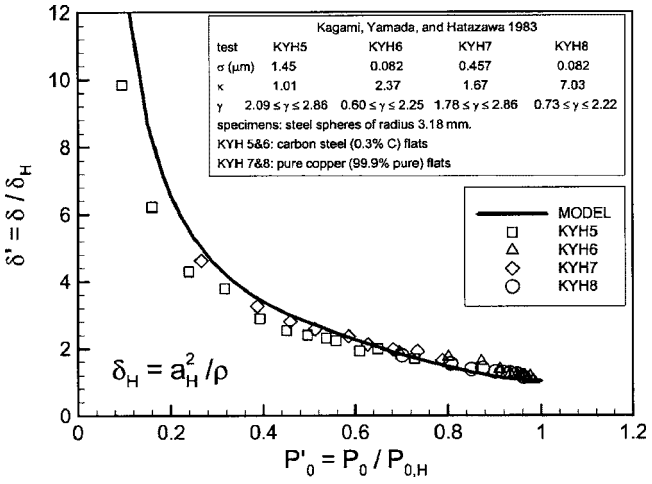

Fig. 9 Comparison between present model and experimental data, compliance

Additionally, an analytical model has been developed to predict TCR of spherical rough surfaces in gaseous environments by the same authors using the general pressure distribution, Eq. (11), and very good agreement was observed with experimental data [20].

To verify the proposed model, the radius of the contact area and the compliance predicted by the model are compared with experimental data collected by Tsukada and Anno (TA) [21], Greenwood et al. (GJM) [17], and Kagami et al. (KYH) [16]. The experimental arrangement contains a smooth sphere placed in contact with a rough plane. The contact area was made visible by depositing a thin layer of copper [17] or an evaporated carbon film and a lamp black film [16]. The contact radii were measured using a metallurgical microscope. Due to the measurement method, the experimental data may contain a relatively high uncertainty particularly at light loads or very rough surfaces since it involved some degree of judgment. Ranges of nondimensional parameters α, κ, and γ covered by the experimental data are shown in Fig. 7. The experimental data include contact between similar (steel-steel) and dissimilar (steel-copper) materials and cover a relatively wide range of load, roughness, and radius of curvature.

The proposed relationship for a_L, Eq. (15) is compared with the data, more than 160 data points, 26 sets, in Fig. 8. The present model shows the trend of the data over the entire range of the comparison. Specimen materials, roughness, and radius of curvature for data sets are listed in Fig. 7. The RMS difference between the proposed expression and the data is approximately 7%.

Greenwood et al. [17] plotted the ratio a_L/a_H predicted by the GT [10] model as a function of α against KYH [16] and their data. They selected two values of the nondimensional parameter μ=4 and 17 arbitrarily, which bracket most practical surfaces [17], to cover these data. In [17], the data showed a large scatter and did not fall within the two curves. Greenwood et al. attributed the observed discrepancy to the experimental difficulties of measuring the contact radius. They also stated that the KYH data did not correlate particularly well with the roughness parameter α. However, as shown in Fig. 8, such a discrepancy has not been encountered in this study.

Kagami et al. [16] also measured the compliance, as defined in Eq. (18), between a smooth steel sphere and rough steel and copper plates. They collected more than 40 data points, two steel-steel and two steel-copper sets. Figure 9 shows the comparison between the present model, Eq. (19) and the KYH compliance data.

The nondimensional parameter P_0' has been used throughout the comparison with experimental data instead of using α and κ. As shown, P_0' does a good job for normalizing the data. P_0' is a meaningful measure that indicates the effect of roughness. As it approaches unity the effect of roughness becomes negligible. Moreover, P_0' contains both α and κ; thus it can be concluded that P_0' is the key parameter that controls the spherical rough solution.

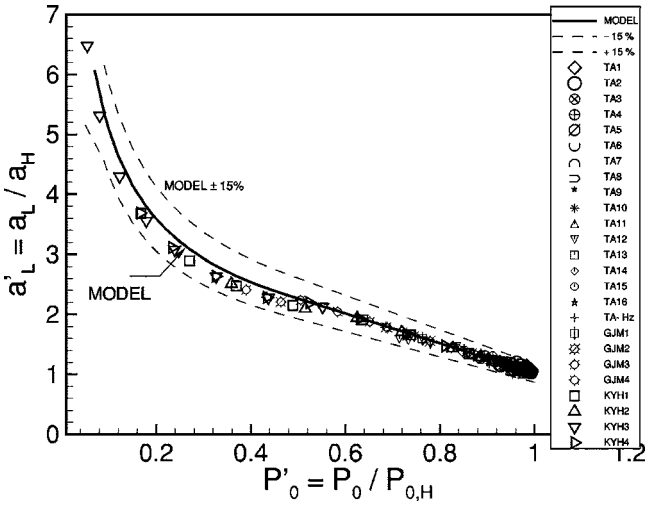

Fig. 8 Comparison between present model and experimental data, contact radius

Summary and Conclusion

The mechanical contact of spherical rough surfaces is studied and a new model is developed. The deformations of surface asperities are considered to be plastic and the bulk deformation is assumed to be within the elastic limit. A closed set of governing equations is derived and solved numerically. It is shown that as roughness approaches zero the predicted pressure distribution approaches the Hertzian contact pressure.

A general pressure distribution is proposed that encompasses all spherical rough contacts including the Hertzian limit. The maximum contact pressure is observed to be the key parameter that specifies the contact pressure distribution.

The results of the analysis are curve-fitted and compact correlations are proposed for calculating the maximum contact pressure, the radius of the contact area, and bulk deformations.

The contact radius and compliance predicted by the model are compared against more than 200 experimental data points collected by others and good agreement is observed.

Acknowledgments

The authors gratefully acknowledge the financial support of the Centre for Microelectronics Assembly and Packaging, CMAP and the Natural Sciences and Engineering Research Council of Canada (NSERC).

Nomenclature

A = area, m^2
a = radius of contact, m
a'_L = relative contact radius, $\equiv a_L/a_H$
E = Young's modulus, Pa
E' = equivalent elastic modulus, Pa
F = external force, N
H_{mic} = effective microhardness, Pa
P = pressure, Pa
P'_0 = relative maximum pressure, $\equiv P_0/P_{0,H}$
r = radial position, m
Y = separation between mean planes, m

Greek

α = roughness parameter, $\equiv \sigma\rho/a_H^2$
β = radius of summits, m
γ = exponent of general pressure distribution
δ = compliance, m
λ = non-dimensional separation, $\equiv Y/\sqrt{2}\sigma$
μ = non-dimensional parameter, $\equiv 8\sigma\eta\sqrt{2\rho\beta}/3$
ν = Poisson's ratio
ξ = non-dimensional radial position, $\equiv r/a_L$
ρ = radius of curvature, m
σ = RMS surface roughness, μm
κ = non-dimensional parameter, $\equiv H_{\text{mic}}/E'\sqrt{\rho/\sigma}$
ω = deformation, m

Subscripts

0 = value at origin
1, 2 = surface 1 and 2
a = apparent, asperity
b = bulk
H = Hertz
r = real

References

[1] Johnson, K. L., 1985, *Contact Mechanics*, Cambridge University Press, Cambridge, UK.
[2] Williamson, J. B., Pullen, J., and Hunt, R. T., 1969, "The Shape of Solid Surfaces," Surface Mechanics, ASME, New York, 1969, pp. 24–35.
[3] Whitehouse, D. J., 1994, *Handbook of Surface Metrology*, Institute of Physics Pub., Bristol.
[4] Cooper, M. G., Mikic, B. B., and Yovanovich, M. M., 1969, "Thermal Contact Conductance," Int. J. Heat Mass Transfer, **12**, pp. 279–300.
[5] Greenwood, J. A., and Williamson, B. P., 1966, "Contact of Nominally Flat Surfaces," Proc. Phys. Soc., London, Sect. A, **295**, pp. 300–319.
[6] Chang, W. R., Etison, I., and Bogy, D. B., 1987, "An Elastic-Plastic Model for the Contact of Rough Surfaces," ASME J. Tribol., **109**, pp. 257–253.
[7] Zhao, Y., Maietta, D. M., and Chang, L., 2000, "An Asperity Model Incorporating the Transition from Elastic Deformation to Fully Plastic Flow," ASME J. Tribol., **122**, pp. 86–93.
[8] Tabor, D., 1951, *The Hardness of Metals*, Oxford University Press, Amen House, London E.C.4, UK.
[9] Archard, J. F., 1953, "Contact and Rubbing of Flat Surface," J. Appl. Phys., **24**, pp. 981–988.
[10] Greenwood, J. A., and Tripp, J. H., 1967, "The Elastic Contact of Rough Spheres," ASME J. Appl. Mech., **89**, pp. 153–159.
[11] Persson, B. N. J., 2000, *Sliding Friction Physical Principles and Applications*, Springer, Berlin, Germany.
[12] Greenwood, J. A., and Wu, J. J., 2001, "Surface Roughness and Contact: An Apology," *Meccanica*, Kluwer Academic Publishers, 36, pp. 617–630.
[13] Majumdar, A., and Bhushan, B., 1991, "Fractal Model of Elastic-Plastic Contact Between Rough Surfaces," ASME J. Tribol., **113**, pp. 1–11.
[14] Gladwell, G. M. L., 1980, *Contact Problems in the Classical Theory of Elasticity*, Alphen aan den Rijn: Sijthoff and Noordhoff, The Netherlands, Germantown, Maryland, USA.
[15] Mikic, B. B., and Roca, R. T., 1974, "A Solution to the Contact of Two Rough Spherical Surfaces," ASME J. Appl. Mech., **96**, pp. 801–803.
[16] Kagami, J., Yamada, K., and Hatazawa, T., 1983, "Contact Between a Sphere and Rough Plates," Wear, **87**, pp. 93–105.
[17] Greenwood, J. A., Johnson, K. L., and Matsubara, M., 1984, "A Surface Roughness Parameter in Hertz Contact," Wear, **100**, pp. 47–57.
[18] Bahrami, M., 2004, "Modeling of Thermal Joint Resistance for Rough Sphere-Flat Contact in a Vacuum," Ph.D. thesis, University of Waterloo, Dept. of Mech. Eng., Waterloo, Ontario, Canada.
[19] Bahrami, M., Culham, J. R., and Yovanovich, M. M., 2004, "Thermal Contact Resistance: A Scale Analysis Approach," ASME J. Heat Transfer, **126**, pp. 896–905.
[20] Bahrami, M., Culham, J. R., and Yovanovich, M. M., 2004, "Thermal Joint Resistance of Non-Conforming Rough Surfaces with Gas-Filled Gaps," J. Thermophys. Heat Transfer, **18**, pp. 326–332.
[21] Tsukada, T., and Anno, Y., 1979, "On the Approach Between a Sphere and a Rough Surface (1st. Report-Analysis of Contact Radius and Interface Pressure," J. Jpn. Soc. Precis. Eng., **45**, pp. 473–479.